Establishing effective criteria to link atomic and macro-scale simulations of dislocation nucleation in FCC metals

†N. J. Burbery[1], R. Das [1], W.G. Ferguson[2], G. Po[3], N. Ghoniem[3]

[1]Department of Mechanical Engineering, University of Auckland, Auckland, New Zealand.
[2]Department of Chemical and Materials Engineering, University of Auckland, Auckland, New Zealand.
[3]Mechanical and Aerospace Engineering Department, Department of Engineering, University of California, Los Angeles 1597, United States of America

†Presenting and corresponding author: nbur049@aucklanduni.ac.nz

Abstract

Processes at fundamental length scales contribute collectively, in a statistical manner, to the macro-scale effects observed at length scales several orders of magnitude higher. To derive useful quantities pertaining to real material properties from atomic scale simulations, it is critical to evaluate the cumulative effect of multiple atomic-scale defects at the 'meso'- and 'micro'- scales. This study aims to develop a phenomenological model for atomic scale effects, which is a critical step towards the development of a comprehensive meso-scale simulation framework. In moderate loading conditions, dislocations in FCC metals are dictated by thermally activated processes that become energetically favourable as the stress approaches a threshold value. The nudged elastic band technique is ideal for evaluating the energetic activation parameters from atomic simulations, in order to evaluate the stress, temperature and rate dependence of a process. On this basis, a constitutive mathematical model is developed for simulations at the meso-scale with respect to the atomic activation parameters, to evaluate the critical (local) shear stress threshold. Once models are established for multiple effects, such as dislocation junction formation, cross-slip, and nucleation, the threshold temperature and stress for a transition between different effects can be evaluated. For example, the threshold temperature can be evaluated during heating, beyond which an immobilised dislocation in a junction will be activated for cross-slip and will shift into an adjacent mobile slip system. This is useful to predict the rate-limiting dislocation process at each simulation timestep, by evaluating the simulation condition-dependent criteria. Additional criteria variables for the constitutive models include properties of the dislocation, the grain boundary and the material's chemical and elastic properties. Multi-scale modelling from a lower-scale basis is inherently limited by a reduction in the degrees of freedom required to enable large scale simulations, constrained by computational limits. To address this, we intend to use hierarchical multi-scale linking by iteratively updating the constitutive model parameters until the meso-scale method is capable of reproducing atomic scale dislocation effects. The resultant meso-scale method will be useful to study multi-dislocation interactions, which are capable of driving high-stress effects such as dislocation nucleation under low applied stresses, due to stress-concentration in dislocation pile-ups at interfaces. This study contributes to the development of a 'fundamental basis' to inform macro-scale models that can provide significant insights about the effect of dislocation microstructure evolution during plastic deformation.

Keywords: Multi-scale computer simulations, dislocation dynamics, FCC metals, polycrystalline plasticity, activation parameters

1.0 Introduction

Dislocations act as a “weak point”, defining the elastic limit and subsequent ductility of crystalline materials, such as FCC metals [Zbib and Khraishi (2005); Po, Mohamed et al. (2014)]. Due to their high mobility at low stress and temperature, once dislocations are activated they act as the primary crystal defects for mediating plastic deformation. Dislocations are atomic bond defects with a core region that is fundamentally defined by the sub-nano scale burgers vector. However, dislocations contribute to mechanical properties via multi-dislocation interactions in a cumulative statistical manner up to ~100 μm [Po, Mohamed et al. (2014)]. Hence, to fully understand the characteristics of dislocations for modelling and prediction, it is critical to utilise a multi-scale approach to evaluate the inter-atomic mechanisms and the inter-dislocation effects [Ghoniem†, Busso et al. (2003)]. Molecular dynamics (or MD) simulations are an ideal tool for developing a conceptual and constitutive modelling framework for the atomic processes which are fundamental to the macroscopic properties seen in real materials. MD is inherently limited to very small size and time simulations by computational requirements, so constitutive models need to be applied in micro-meso scale methods such as dislocation dynamics (DD) to evaluate cumulative effects [Po, Lazar et al. (2014)].

Dislocation-mediated deformation is strongly influenced by thermally activated nucleation, especially when confined within a nano-crystalline material with a grain size less than ~0.1 μm [Zhu, Li et al. (2008)]. Recent developments in computational methods have been developed to simulate the minimum energy path (MEP) for an atomic transition, which indicates the activation energy (Ea). The nudged elastic band method (NEB) is a popular method which obtains the MEP by minimizing the potential energy of transition states interpolated between input initial and end states [Henkelman, Uberuaga et al. (2000)]. The stress dependence of the activation energy (E_a) is known as the activation volume (Ω). Ω can be evaluated by calculating the MEP between identical initial and final atomic configurations, but with various externally applied loads [McPhie, Berbenni et al. (2012)]. The fundamental activation properties (E_a and Ω) are time-stress and temperature independent [Voter, Montalenti et al. (2002)]. Assuming the atomic mechanism is independent of simulation scale, the activation parameters are hence ideal for linking multi-scale simulation methods. On this basis, the thermal activation parameters can be used to establish a constitutive model for predicting the threshold for nucleation, as a function of two known parameters (from stress, temperature and/or strain rate) [Zhu, Li et al. (2008)]. This study establishes a constitutive model using transition state theory to provide a critical contribution for atomic-informed meso-scale computer simulations.

2.0 Methods

Single crystals of pure FCC aluminium were simulated using molecular static simulations, with an embedded atom method (EAM) inter-atomic potential provided by [Mishin, Farkas et al. (1999)]. This EAM potential was chosen because it efficiently simulates the stacking fault energies and elastic properties of pure FCC Al. Single crystals are initialised without defects and with periodic boundaries in all dimensions, to represent an ‘infinite single crystal’. The length in the ‘y-axis’ was defined to be greater than 30nm, and the ‘x-‘ and ‘y-‘ axes were 10 lattice units each, in agreement with prior simulations of dislocation nucleation [Tschopp and McDowell (2007; Sangid, Ezaz et al. (2011; Tucker and McDowell (2011)]. Loading was applied along the [110] close-packed slip direction via constant applied uniaxial strain in the y-direction, so the single crystal was oriented as shown in Figure 1. A fully-dense, minimum energy state was obtained using the conjugate gradient minimization method [Štich, Car et al. (1989)]. The crystal was temperature-rescaled to 50K and temperature-pressure equilibrated by Nose-Hoover thermo-barostat and 0 Bar pressure [Nosé (1984; Hoover (1986)]. The crystal orientations and exact dimensions can be most easily understood schematically, by referring to Figure 1. Note that atomistic "imaging" of simulation states is performed using AtomEye visualisation tool [Li (2003)], and atoms are coloured by either: (a) potential energy or (b) centro-symmetry bond parameter (P_{csym}) [Kelchner, Plimpton et al. (1998)].

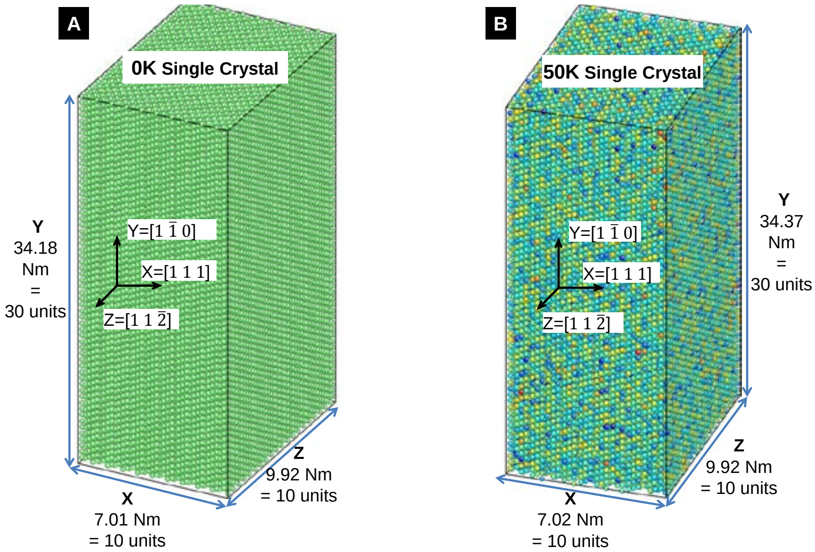

Figure 1: Dimensions and crystal orientations of pure FCC aluminium: A) at 0K; B) at 50K (Note: atoms coloured according to potential energy)

A dislocation was generated in the simulation volume at 50K, by applying a constant rate tensile strain in the $[1\bar{1}0]$ direction at a rate of $5.0e^{8}$ s^{-1}, with outputs provided every 0.1ps for restarting and visualisation. By selectively filtering atoms according to the P_{csym}, the first interval was identified containing atoms with high P_{csym}, to indicate the initiation of crystal slip. From the associated restart file at this point, an instantaneous reverse strain was applied by rescaling the simulation y-dimension in a fashion, followed by immediate rapid quenching to 1K. The atomic velocity and kinetic energy was then reduced to 0 (i.e., 0K) and the simulation energy was minimized by the conjugate-gradient method [Štich, Car et al. (1989)], with an energy tolerance of $1.0e^{-6}$ eV. This energy tolerance matches that used by a similar prior study, which retains a "metastable" dislocation loop at 0K [McPhie, Berbenni et al. (2012)]. By iteratively testing multiple the reverse strain magnitudes, the exact final simulation stress-strain state was identified which would establish a stable dislocation loop after minimization at 0K. This elaborate process of heating, stressing and quenching was necessary to form a single stable "loop", as multiple dislocations will simultaneously nucleate above the yield stress at 0K. This method was used to establish the end-state atomic configuration for NEB simulations. The initial state was created by following an identical heat – stress - quench minimization protocol, however the initial strain is much lower. Specifically, the initial state was chosen so that it relaxes to 0 GPa, after the reverse strain is applied.

NEB simulations were performed using the "replica" library available within the LAMMPs code [Plimpton (1995)] to an energy tolerance of $1e^{-6}$ eV (to match the previously utilised tolerance). To obtain a useful result, it is critical that the simulation volumes of the initial and final states are identical. To achieve this, the initial state dimensions were re-scaled to match the final state dimensions. To study the stress-dependence of the energy threshold required for dislocation nucleation, it was necessary to repeat NEB simulations at various stresses. This was achieved by utilising an additional stage of incrementally increasing strain in the y-dimension immediately following the first stage of quench-minimization. An additional stage of minimization was also applied. Finally, NEB simulations were performed between the identically dimensioned initial defect-free state and the end state containing a dislocation loop. *Ea* for dislocation nucleation was evaluated for each stress state. To evaluate whether there was any relationship between the *Ea*, activation volume, temperature, yield strength and strain rate, dynamic simulations were performed at various temperatures from 0K – 1200K, and at strain rates between 5.0e7 – 5.0e9 s-1. Hence, the temperature and rate dependent stress-strain curves were obtained. For constitutive modelling, data analysis, regression modelling and mathematical validation were performed with Microsoft Excel.

3.0 Results and discussion

3.1 Key thermal and mechanical properties for predictive modelling

It is critical to evaluate the threshold disorder temperature ($T_{disorder}$) which is accurate for the inter-atomic potential used to represent the material properties in atomic simulations. $T_{disorder}$ can be described as the threshold beyond which the yield stress for dislocation nucleation deviates pronouncedly from a linear relationship. The characteristic $T_{disorder}$ properties of single crystal aluminium, using EAM potential from [Mishin, Farkas et al. (1999)] with the crystal orientation shown in Figure 1 is derived from a plot of yield stress as a function of temperature in Figure 2.

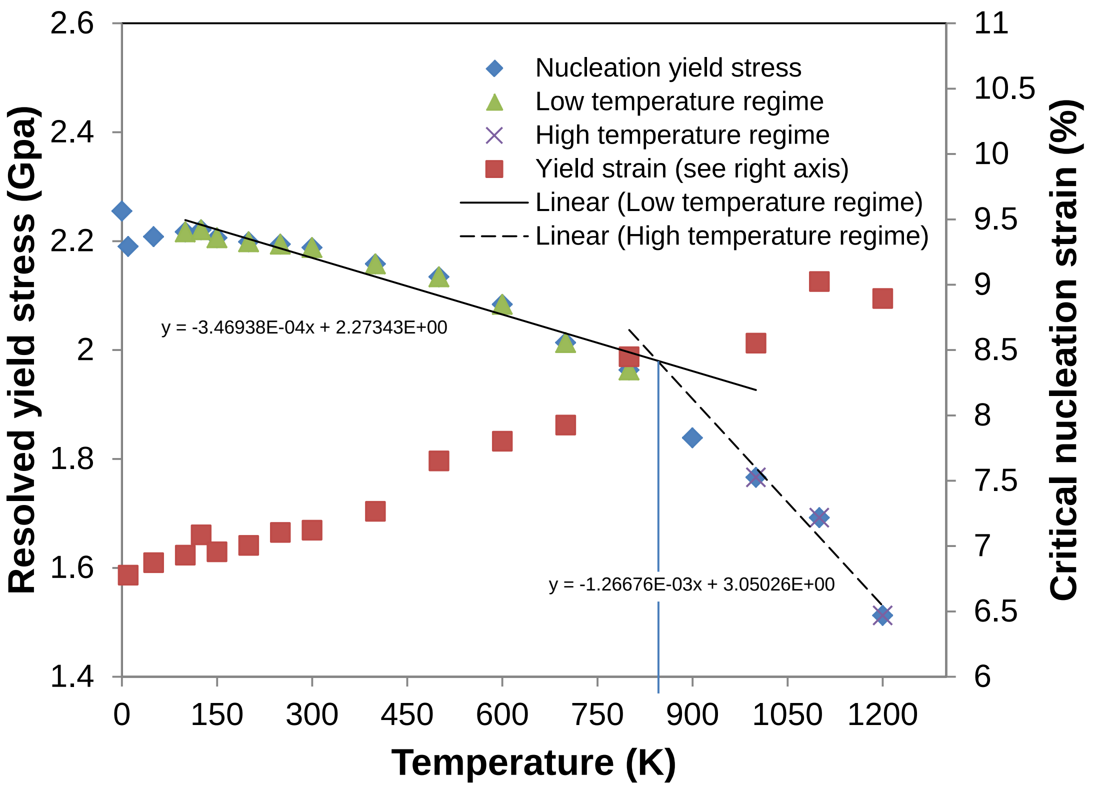

Figure 2: Temperature-dependent strength of single crystal Al in uniaxial tension

Figure 2 demonstrates that the Al atomic potential [Mishin, Farkas et al. (1999)] exhibits approximately linear temperature-strength relationships under strain rates accessible within atomic simulations. Note that the square data points representing yield strain correspond with the y-axis on the right of the figure. The results also provide a valuable analogue for the energy-based constitutive models, derived in later sections from NEB simulations.

Previous detailed analysis of the thermal decomposition temperature, identified that pure FCC aluminium will begin to destabilize at approximately 867.7 K [Nguyen, Ho et al. (1991)]. Referring to Figure 2, there are clearly two linear stress-temperature regimes. The intersection point between the extrapolated curves obtained by simple linear regression indicates the transition temperature, which lies directly between 800K and 900K. Analytical evaluation of the temperature at which the regression curves intersects, results in an exact decomposition temperature of 844.54K, which is in very close agreement with the results obtained in [Nguyen, Ho et al. (1991)]. The critical strain also appears to deviate from a linear trend above 800, with a significant reduction at 900K. Beyond this temperature, the critical strain increases sharply despite a reduction in the yield stress, confirming that the material has distinctly altered elastic properties above 800K.

3.2 Characteristics of homogeneous dislocation nucleation

This section will demonstrate the transitional atomic mechanism for dislocation nucleation from a homogeneous, defect free single crystal at 0K and will evaluate the critical athermal activation parameters (i.e., 0 GPa stress and 0K). These parameters are key constant parameters, which form the fundamental basis of constitutive modelling based on thermal activation parameters [Zhu, Li et al. (2008)]. This is most clearly shown by visualising the generation of defect atoms in transitional atomic states, which are identified by the centro-symmetry bond coefficient [Kelchner, Plimpton et al. (1998)]. The transition states and energy barrier are seen in Figure 3.

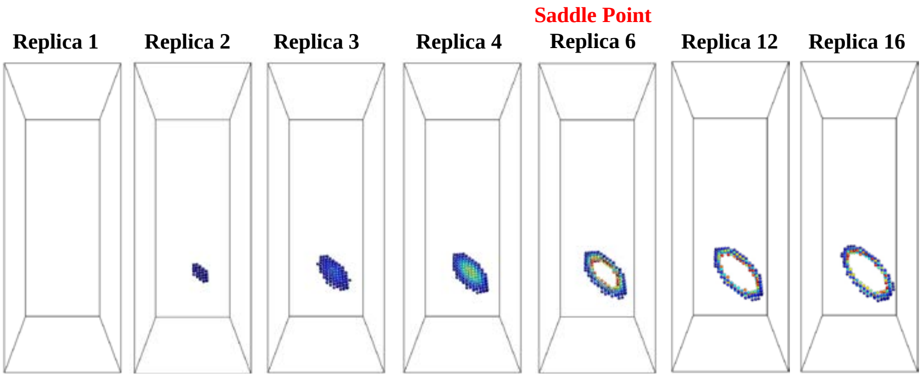

Figure 3a.: Generation of defect atoms during dislocation nucleation transition

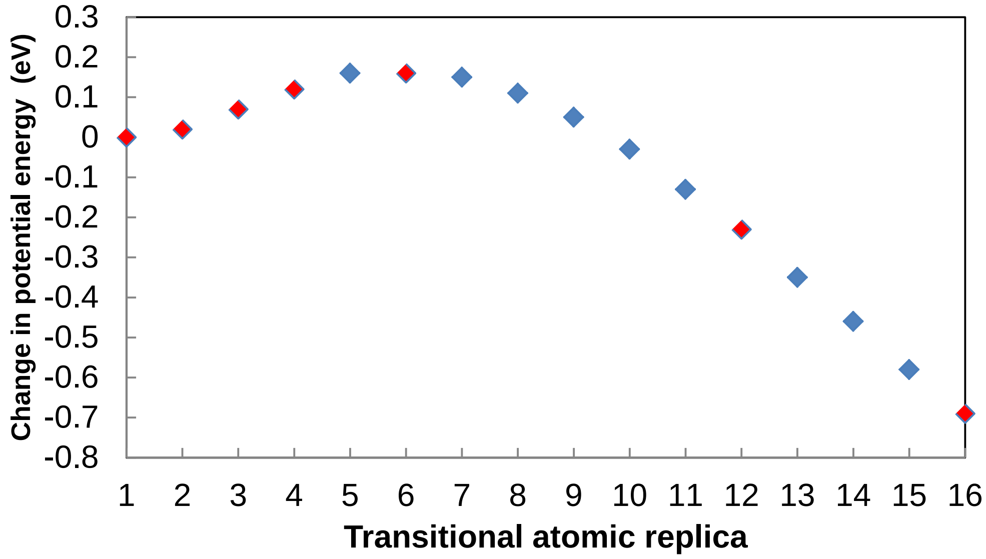

Figure 3b.: Minimum energy barrier for near-athermal dislocation nucleation

Figure 3: transition for dislocation nucleation from Nudged elastic band simulation at 0K and at 2.22 GPa (near athermal yield stress)

Figure 3 shows the results of an NEB simulation between the initial defect free state and final state containing a single full dislocation loop at approximately 2.22 GPa. The process begins with the generation of a Shockley Partial dislocation with a Burgers vector of $[\bar{1}1\bar{2}]$, and magnitude of 1.672Å. Close inspection shows that nucleation is initiated as fundamental atomic-scale vibration in 2 or 3 atoms, resulting in the minor bond disruption of 9 atoms in 2 adjacent $(\bar{1}1\bar{1})$ planes. There is a substantial reduction in potential energy, which likely corresponds with the relaxation of the elastic strain energy in all non-defect atoms in the volume. Note that this also corresponds with a very minor reduction in shear stress of ~0.06GPa, however this change is considered negligible. The forward energy barrier approaches zero as the stress increases above 2.2 GPa, which is why nucleation can proceed without thermal input above the athermal stress-strain limit.

It is interesting to note that the dislocation loop is not at a maximum size at the saddle point. However, this is probably explained because the saddle point involves the energy jump required to nucleate the trailing partial dislocation. For this reason, the potential energy of the defected atoms is at the highest in this replica. This also indicates that the elastic strain and stacking fault energies decrease beyond this point.

3.3 E_a for homogeneous nucleation as a function of stress

The E_a for dislocation nucleation was calculated for single crystals with a residual shear stress of between -0.04 GPa to 2.19 GPa. The stress-dependence is most clearly shown graphically according to Figure 6.

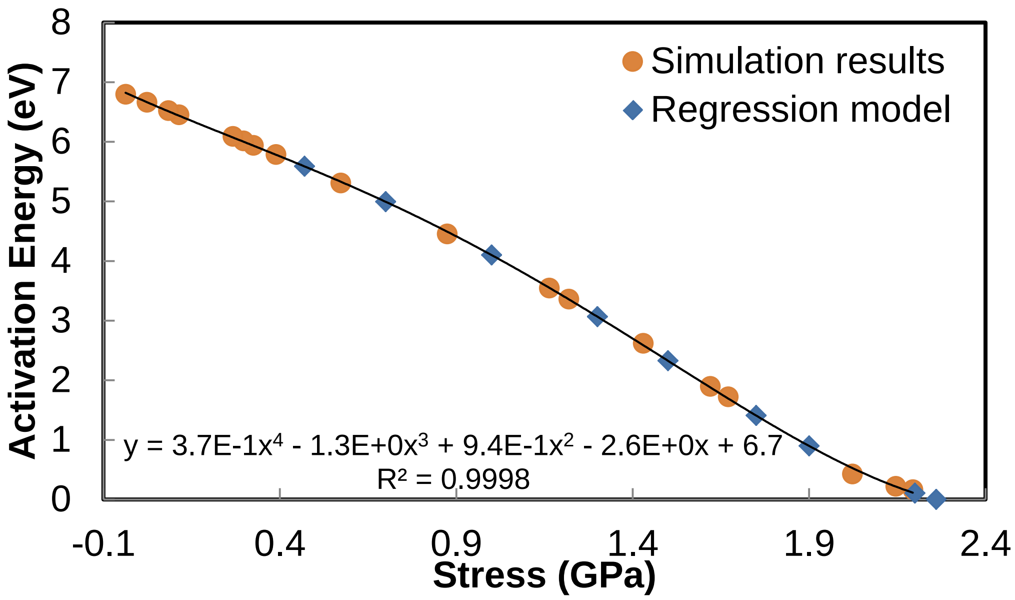

Figure 4: E_a for dislocation nucleation as a function of resolved shear stress

Figure 6 shows a nearly linear relationship exists between stress and E_a until approximately 1.4GPa. Beyond this point, the relationship is non-linear and approaches a more 'exponential shape'. The critical stress with an E_a of 0.0eV was extrapolated from the data using a 4th order polynomial regression curve, fitted to the simulation data with an R^2 value of 0.9998. Note that only 1 SF is shown in figure due to space limitations. Accordingly, the critical athermal resolved shear stress for spontaneous dislocation nucleation is exactly 2.26 GPa. This is another critical parameter that will be used for the constitutive modelling in the next section.

These results are also ideal for an explicit evaluation of the activation volume Ω, according to the standard thermodynamic relationship shown in Equation 1:

$$\Omega = \left(\frac{\partial \Delta E_A}{\partial \sigma} \right)_{T,P} \tag{1}$$

According to Equation 1, the activation volume can be very simply evaluated from the stress dependent E_a at constant temperature and hydrostatic pressure. Temperature is, by definition of the NEB procedure, exactly 0K. The hydrostatic pressure is 0 Bar, due to the algorithms used to define the uniaxial loading and with damping to reduce fluctuations from the Hoover barostat [Hoover (1986)]. If evaluated from total data range, the Ω is 4.9e^{-28} J/Pa. For stresses greater than 2.1 GPa, the Ω is 2.5e^{-28} J/Pa and for stresses less than 2.1 GPa and greater than 0.8 GPa, the Ω is 5.66e^{-28} J/Pa. The activation volume is a critical fundamental parameter that can has been correlated with the strain rate dependence of nucleation with simulations [Deng and Sansoz (2010)] and experiments [Asaro and Suresh (2005)].

3.4 Constitutive model for temperature – strain rate dependent yield stress

The activation energy, E_a, is typically used to directly evaluate the thermal effect on mechanical properties, and is directly correlated with the temperature according to Equation 2:

$$E_{a,T} = \left(1 - \frac{T}{T_{disorder}}\right) E_{a,0K} \text{ [Zhu and Li (2010)]} \tag{2}$$

In combination with the activation volume, *Ω*, the stress can be evaluated according the simplified, modified version of the relationship derived by Zhu et al. [Zhu and Li (2010)]:

$$\sigma = \left(\sigma_{athermal} - \ln \frac{k_b T N \nu_0}{E \dot{\varepsilon} \Omega}\right) \text{ [Zhu and Li (2010)]} \tag{3}$$

where $\sigma_{athermal}$ is the critical shear stress at 0K, k_b is the Boltzmann constant, $N\nu_0$ is the number of transitions attempted per second, E is the Young's modulus and $\dot{\varepsilon}$ is the strain rate. Unfortunately, although this method is based on fundamental theoretical physics, it is dependent on an accurate evaluation of the exact context – dependent value of *Ω* and is typically flawed by a biased "prediction" of $N\nu_0$ [Zhu, Li et al. (2009)]. As the strain rate decreases and the temperature decreases, the stress is influenced in a multiplicative manner. Hence, the cumulative effects should be significant when comparing 0K atomic simulations at 5.0e^{8} s^{-1} with experiments which are typically at strain rate <1s^{-1} and at 298K. Thermally activated dislocation nucleation exhibits a physics-based correlation the yield stress and the strain rate according to:

$$\Omega = \frac{k_b T}{m\sigma} \text{ [Asaro and Suresh (2005)]} \tag{4}$$

where *m* is the strain-rate sensitivity exponent. If *Ω* is assumed stress-independent (i.e., Figure 6 is linear), it is possible to evaluate the temperature dependence by re-arranging Equation 4 and solving for *m* at $\dot{\varepsilon}_{athermal}$ and $\sigma_{athermal}$. The critical resolved shear stress at a given $\dot{\varepsilon}$ and *T* is then predicted with the well-established formula:

$$\frac{\sigma}{\sigma_{Athermal}} = \left(\frac{\dot{\varepsilon}}{\dot{\varepsilon}_{Athermal}}\right)^m \tag{5}$$

Using Equation 5, the yield stress is predicted as a function of temperature at a variety of strain rates between 5.0×10^{8} s^{-1} - 500 s^{-1}. The results are then compared with dynamic simulation results at strain rates of 5.0×10^{8}, 1.0×10^{8}, and 1.0×10^{7} s^{-1}. Unfortunately, it was impossible to go to lower strain rates, due to inherent computational limitations of atomic simulations. Refer to Figure 7.

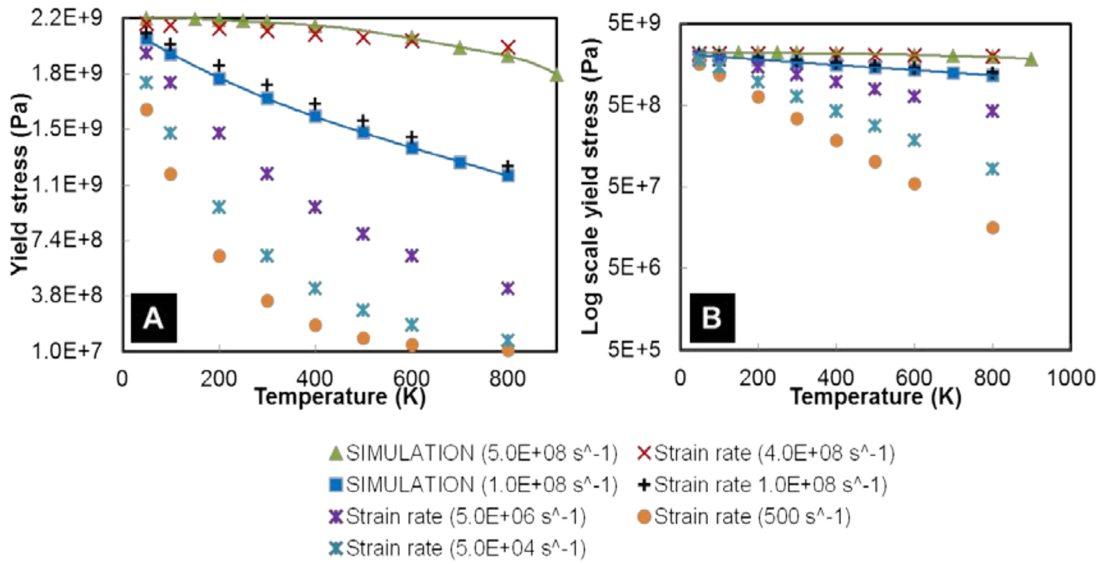

Figure 5: Comparison of yield stress-T curves at different strain rates between MD simulations and model predictions: (A) Yield stress in Pa, (B) Logarithmic scale yield stress

Figure 7 shows solid lines interpolated from the yield stress obtained with simulations at constant strain rate, corresponding with the peak stress value obtained prior to the first dislocation nucleation event. The data points without corresponding solid lines are values calculated directly using Equation 5. Figure 7B is identical to Figure 7A, however with a logarithmic scale on the y-axis. Figure 7B provides a clear demonstration that the temperature dependence does not reach an asymptote at $T > 600\text{K}$ and $\dot{\varepsilon} > 5.0 \times 10^4$ s-1.

The results in Figure 7 demonstrate remarkable consistency between the simulated and analytically predicted yield stress, as a function of strain rate and temperature between $1.0 \times 10^7 \le \dot{\varepsilon} \le 5.0 \times 10^8$ and up to 800K. This is not coincidental, as the temperature dependence is significantly strain-rate dependent, as demonstrated by the significant difference between $\dot{\varepsilon} = 5.0 \times 10^8$ and $\dot{\varepsilon} = 5.0 \times 10^7$ by 1 order of magnitude at 800K. This provides an extremely significant timescale link between atomic simulation (<100µs) and experiments (>1ms), and a valuable constitutive model.

3.5 Effectiveness of model at low strain rate and significance

This section will discuss the suitability of the model derived from an energy-based criterion to effectively predict the rate-dependence of yield stress and the significance of this for atomic simulation studies.

The primary challenge of simulation-based studies, is establishing an effective link between the idealised, theoretical model and the real-world properties. Fundamentally, energy criteria are ideal, as they are pure thermodynamic values that are time-size-temperature independent, and can also be used to explain complex “real-world” non-ideal material properties by accounting for defect energies. However, this requires a consistent mechanism when effects of strain rate and material defects are included. For example, due to time-dependent effects, “slow” processes such as mechanical creep may not be observed in atomic simulations, because they require longer timeframes (> 1s). However, it can be assumed to be a very good approximation of homogenous dislocation nucleation processes, such as is consistently observed in nano-indentation experiments [Lorenz, Zeckzer et al. (2003; Zhao, Ma et al. (2012)].

The model obtained corresponds very well with previous studies [Asaro and Suresh (2005; Zhu, Li et al. (2008; Deng and Sansoz (2010; Zhang, Liu et al. (2013)], and there is evidence that the energy-based criterion is effective for atomic-experimental timescale linking [Zhu, Li et al. (2008)].

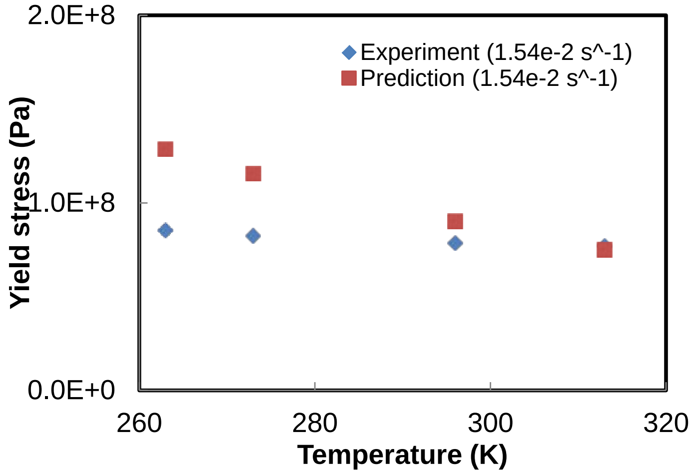

6

Figure 6a: Small temperature range comparison of experiment and predicted results

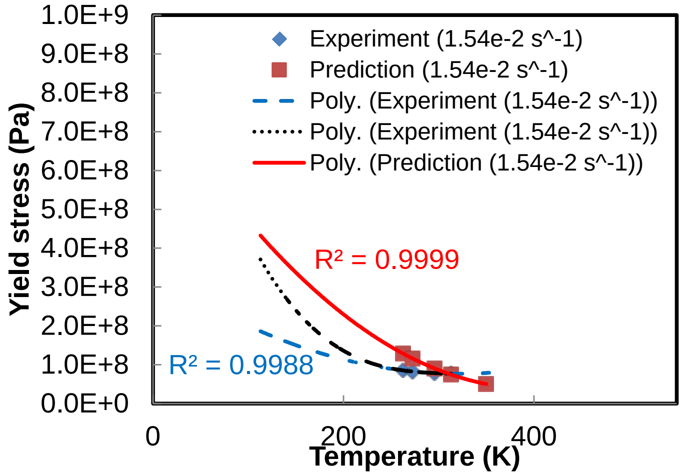

Figure 7b: Extrapolation of polynomial regression models showing results may diverge

Figure 8: Comparison of predicted and experimental flow stress at $\dot{\varepsilon} = 1.54 \times 10^{-2}$ s^{-1}

Although the accuracy of the model derived in this paper is very good for all the testable strain rates, it cannot be validated at low strain rates (i.e., $\dot{\varepsilon} < 5.0 \times 10^{6}$) by the same atomic simulation approach, as explained in the introduction. The flow stress provides an analogue for the experimental nucleation yield stress [Deng and Sansoz (2010)]. Hence, Figure 8 validates the model by comparing the flow stress as a function of temperature from an experimental study with pure FCC Al [Rosen and Bodner (1967)] with the predicted yield stress at a strain rate of $\dot{\varepsilon} = 1.54 \times 10^{-2}$ s-1. This provides an indication of the validity of the model for low strain rate regimes by comparing with results in the literature. Note: this is limited due to the small data set available experimentally [Rosen and Bodner (1967)]. The results are very consistent around the temperature of 300K. However, the results appear to diverge slightly as the experimental temperature decreases below 0°C. To test the divergence, the results are backwards extrapolated with regression models, showing that a 2nd order model will exhibit fairly significant divergence as $T \to 0K$. However, the result is remarkably consistent considering that the simulation results at $\dot{\varepsilon} = 5.0 \times 10^{8}$ s-1 and

300K is 28 times greater than the experimental result. The result is a very promising time and size link from atomistic to experimental results.

4.0 Conclusions

This study demonstrates that the non-elastic mechanical properties of crystalline materials can be defined by the atomic-scale crystal defect processes, which are driven by the thermal and mechanical limits. This paper shows that the yield stress (mechanical limit) in a defect-free single crystal can be correlated with the activation energy for dislocation nucleation. The activation energy is hence used as a fundamental-basis to model the temperature-dependence (thermal limits). More significantly, this paper demonstrates that the stress-dependence of the activation energy (i.e., the activation volume) can be used to accurately predict the effect of strain rate on the temperature-dependence of mechanical strength. In other words, this paper shows that a fundamental energy criterion from atomistic simulations can be used to derive an effective constitutive model for temperature- and rate- dependent thermo mechanical properties! This is a critical insight, because it enables a timescale link between atomistic simulations at very high strain rates ($\dot{\varepsilon} > 5.0\times10^{6}$ s^{-1}), and macro-scale simulations and/or experiments.

5.0 References

Asaro, R. J. and S. Suresh (2005). "Mechanistic models for the activation volume and rate sensitivity in metals with nanocrystalline grains and nano-scale twins." Acta Materialia **53**(12): 3369-3382.

Deng, C. and F. Sansoz (2010). "Effects of twin and surface facet on strain-rate sensitivity of gold nanowires at different temperatures." Physical Review B **81**(15): 155430.

Ghoniem†, N. M., E. P. Busso, et al. (2003). "Multiscale modelling of nanomechanics and micromechanics: an overview." Philosophical Magazine **83**(31-34): 3475-3528.

Henkelman, G., B. P. Uberuaga, et al. (2000). A climbing image nudged elastic band method for finding saddle points and minimum energy paths. The Journal of Chemical Physics. **113:** 9901-9904.

Hoover, W. G. (1986). "Constant-pressure equations of motion." Physical Review A **34**(3): 2499-2500.

Kelchner, C. L., S. J. Plimpton, et al. (1998). "Dislocation nucleation and defect structure during surface indentation." Phys Rev B: Condens Matter and Mater Phys **58**(17): 11085-11088.

Li, J. (2003). "AtomEye: an efficient atomistic configuration viewer." Modelling and Simulation in Materials Science and Engineering **11**(2): 173.

Lorenz, D., A. Zeckzer, et al. (2003). "Pop-in effect as homogeneous nucleation of dislocations during nanoindentation." Physical Review B **67**(17): 172101.

McPhie, M. G., S. Berbenni, et al. (2012). "Activation energy for nucleation of partial dislocation from grain boundaries." Computational Materials Science **62**(0): 169-174.

Mishin, Y., D. Farkas, et al. (1999). "Interatomic potentials for monoatomic metals from experimental data and ab initio calculations." Physical Review B **59**(5): 3393-3407.

Nguyen, T., P. S. Ho, et al. (1991). Molecular Dynamics Study of Thermal Disorder in a Bicrystal Model. MRS Proceedings, Cambridge Univ Press.

Nosé, S. (1984). "A unified formulation of the constant temperature molecular dynamics methods." The Journal of Chemical Physics **81**(1): 511-519.

Plimpton, S. J. (1995). "Fast Parallel Algorithms for Short-Range Molecular Dynamics." Journal of Computational Physics **117**(Refer to: http://lammps.sandia.gov): 1-19.

Po, G., M. Lazar, et al. (2014). "Singularity-free dislocation dynamics with strain gradient elasticity." Journal of the Mechanics and Physics of Solids **68**(0): 161-178.

Po, G., M. Mohamed, et al. (2014). "Recent Progress in Discrete Dislocation Dynamics and Its Applications to Micro Plasticity." JOM **66**(10): 2108-2120.

Rosen, A. and S. R. Bodner (1967). "The influence of strain rate and strain ageing on the flow stress of commercially-pure aluminium." Journal of the Mechanics and Physics of Solids **15**(1): 47-62.

Sangid, M. D., T. Ezaz, et al. (2011). "Energy of slip transmission and nucleation at grain boundaries." Acta Materialia **59**(1): 283-296.

Štich, I., R. Car, et al. (1989). "Conjugate gradient minimization of the energy functional: A new method for electronic structure calculation." Physical Review B **39**(8): 4997.
Tschopp, M. A. and D. L. McDowell (2007). "Asymmetric tilt grain boundary structure and energy in copper and aluminium." Philosophical Magazine **87**(25): 3871-3892.
Tucker, G. J. and D. L. McDowell (2011). "Non-equilibrium grain boundary structure and inelastic deformation using atomistic simulations." International Journal of Plasticity **27**(6): 841-857.
Voter, A. F., F. Montalenti, et al. (2002). "EXTENDING THE TIME SCALE IN ATOMISTIC SIMULATION OF MATERIALS." Annual Review of Materials Research **32**(1): 321-346.
Zbib, H. M. and T. A. Khraishi (2005). Dislocation Dynamics. Handbook of Materials Modeling. S. Yip, Springer Netherlands**:** 1097-1114.
Zhang, J. Y., G. Liu, et al. (2013). "Strain rate effects on the mechanical response in multi- and single-crystalline Cu micropillars: Grain boundary effects." International Journal of Plasticity **50**(0): 1-17.
Zhao, J., L. F. Ma, et al. (2012). "Surface dislocation nucleation by wedge indenter contacts." Materials Science and Technology **28**(9-10): 1167-1172.
Zhu, T. and J. Li (2010). "Ultra-strength materials." Progress in Materials Science **55**(7): 710-757.
Zhu, T., J. Li, et al. (2009). "Mechanics of ultra-strength materials." MRS bulletin **34**(3): 167.
Zhu, T., J. Li, et al. (2008). "Temperature and Strain-Rate Dependence of Surface Dislocation Nucleation." Physical Review Letters **100**(2): 025502.